BMC Ophthalmology

RESEARCH

Open Access

Corneal higher-order aberrations and their relationship with choroid in myopic patients

Kaiming Ruan[1,2*†], Dan Cheng[1,2†], Xueying Zhu[1,2], Shiqi Sun[1,2], Fangjun Bao[1,2], Jun Zhu[1,2], Fenfen Li[1,2], Meixiao Shen[1,2*†] and Yufeng Ye[1,2*†]

Abstract

Background To investigate corneal higher-order aberrations (HOAs) and choroidal characteristics in myopic individuals and explore the association between HOAs and choroidal parameters.

Methods Myopic participants were categorized into three groups based on axial lengths (ALs). We compared corneal HOAs, including spherical (Z_4^0), comatic (Z_3^{-1} and Z_3^1), and trefoil (Z_3^{-3} and Z_3^3) aberrations, as well as choroidal vascularity index (CVI) and choroidal thickness (CT). Linear regression analysis was used to assess the relationships among corneal HOAs, CVI, CT, spherical equivalent, and AL.

Results Groups 1, 2, and 3 included 105, 98, and 118 eyes, respectively. Group 3 exhibited lower spherical HOA root mean square and Z_4^0 values than group 1 ($p < 0.05$). Group 1 showed lower Z_3^1 levels than other groups ($p < 0.001$). Groups 1 and 2 had higher mean, central, and I2 vertical CVIs than group 3 ($p < 0.05$). Group 1 had a larger vertical S1 CVI than group 3 ($p < 0.05$). Group 3 had smaller horizontal CVI values in all regions except N2 ($p < 0.05$). Both the mean and CT in all regions decreased as AL increased ($p < 0.001$). The comatic (Z_3^1) and trefoil (Z_3^3) components were predictors of mean horizontal CVI, and the comatic (Z_3^1) component was correlated with both mean vertical and horizontal CT.

Conclusion Longer AL myopic patients exhibited lower absolute values of spherical aberration and horizontal coma. Alterations in choroid in myopic patients correlated with corneal HOAs. Our results suggest a potential connection between the optical quality and ocular perfusion in myopia.

Keywords Myopia, Higher-order aberrations, Choroidal vascularity index, Choroidal thickness

Background

Myopia is a severe global health concern, which is increasingly placing a substantial socioeconomic burden on the public [1]. Holden et al. estimated that by 2050, 49.8% of the global population will have myopia and 9.8% will have high myopia [2]. Additionally, an increased risk of potentially sight-threatening complications are associated with different levels of myopia [3]. For each additional diopter of myopia, the risk of myopic maculopathy, open-angle glaucoma, posterior subcapsular cataract, and retinal detachment increased by 58%, 20%, 21%, and 30%, respectively [3]. Consequently, numerous

†Kaiming Ruan and Dan Cheng contributed equally to this work and shared the first authorship.

†Meixiao Shen and Yufeng Ye contributed equally to this research and shared corresponding authorship.

*Correspondence:
Kaiming Ruan
645312122@qq.com
Meixiao Shen
smx77@sohu.com
Yufeng Ye
yyf0571@mail.eye.ac
[1]National Clinical Research Center for Ocular Diseases, Eye Hospital, Wenzhou Medical University, Wenzhou 325027, China
[2]Wenzhou Medical University, Wenzhou, China

studies have been conducted, both in animal models and in human subjects, to explore interventions for myopia control. These interventions include orthokeratology, soft contact lenses, atropine, and spectacles [1, 4–6]. Previous studies indicated that low-order aberrations increased by optical defocus is a common intervention [7]. Recently, higher-order aberrations (HOAs) have been closely associated with myopia progression, influencing both the development and management of the condition [8]. Understanding the specific characteristics of HOAs is clinically significant, as it helps optimize wavefront-guided excimer laser refractive surgery, tailor custom intraocular lens (IOL) implants, and design effective contact lenses that can potentially slow myopia progression.

HOAs are optical imperfections in the eye that can notbe corrected with traditional optical corrections (such as spectacles or contact lenses), leading to visual distortions and reduced optical quality. There is a disagreement regarding the relationship between HOAs and refractive errors. Some studies have reported a higher level of HOAs in myopic adults than in emmetropic eyes [9], while others have found no significant differences [10]. Moreover, hyperopic eyes exhibit greater HOA root mean square (RMS) than myopic eyes [11]. In addition, some longitudinal studies show a negative association between HOAs and axial elongation [12, 13], In particular, spherical aberration (SA) and coma have an association with the growth of AL [13]. Notably, the distribution of specific HOAs in different refractive errors and its correlated factors would provide valuable insights for myopia management [14, 15]. Further, corneal aberration, which stems from irregularities in the shape of the cornea, was the major contribution to ocular HOAs and exhibited strong correlations with refractive error shift and change in axial length [16].

Vision-dependent mechanisms may play a critical role in the emmetropization of myopic patients [17]. According to this theory, images projected onto the retina, influenced by ocular aberrations, impact retinal dopamine homeostasis, subsequently resulting in a reduction in choroidal blood flow. This decreased choroidal perfusion may contribute to axial myopia through mechanisms involving scleral hypoxia and remodeling of the scleral extracellular matrix (ECM) [18–20].

On the other hand, the choroid, as a regulator of scleral ECM remodeling and eye growth, plays a pivotal role in accommodation [21], which contributes to regulating HOAs to improve the retinal image quality [22]. Furthermore, recent evidence indicates that vascular changes in the choroid serve as early indicators of vision-driven alterations in ocular growth and myopia development [23–25].

The variation in corneal HOAs between people of different refractive errors remains limited, as well as the relationship between corneal HOAs and choroidal changes in myopic patients. Further research is needed to elucidate how specific components of HOAs influence choroidal vasculature, contributing to a more comprehensive understanding of myopia progression and facilitating more effective myopia prevention and management strategies. The current study aimed to characterize corneal HOAs and choroidal structures in patients with varying degrees of myopia and to investigate the association between HOAs and choroidal parameters.

Materials and methods

Study participants

The study protocol followed the principles of the Declaration of Helsinki and was approved by the Ethics Committee of Wenzhou Medical University (approval number: No. KYK2018-29). All individuals were informed about the content and purpose of the study, and their informed consent was obtained prior to the examination. Young myopic patients were prospectively recruited between September 2021 and February 2022 from the Affiliated Eye Hospital of Wenzhou Medical University in Hangzhou, Zhejiang. These patients sought consultation for myopic refractive surgery at our hospital's Refractive Surgery Center.

The inclusion criteria were as follows: healthy individuals aged between 18 and 45 years, BCVA of 20/25 or better, astigmatism within ±2.0 D, and IOP < 21 mm Hg. This age group was chosen because it represents a period when myopia progression has typically stabilized, minimizing confounding variables related to ongoing myopic changes during childhood or age-related degenerative changes in older adults. The exclusion criteria were as follows: presence of other intraocular diseases, such as keratoconus, glaucoma, uveitis, and cataract; various pathologic changes on the myopic fundus or OCT, such as staphyloma, lacquer cracks, and myopic macular degeneration; history of previous eye surgery; use of myopia control measures in the past 6 months (including progressive multifocal lens, orthokeratology lens, etc.) and recent history of wearing contact lenses within 2 weeks. Participants with pupil diameters less than 6 mm in a scotopic environment were also excluded.

Sample size calculations were performed using G*Power software, assuming a medium effect size (Cohen's d = 0.5), 80% power, and an alpha value of 0.05. This indicated that a minimum of 95 participants per group was required to detect significant differences between groups. These calculations ensured that the study was adequately powered to support the reliability of the findings.

Each participant underwent a complete ocular examination, including best-corrected visual acuity (BCVA), autorefractometry, slit-lamp examination, intraocular

pressure (IOP) using a non-contact tonometry (CANNON TX-F), axial length (AL) using an optical biometer (IOL Master 700; Carl Zeiss Meditec, Jena, Germany), Swept source optical coherence tomography (SS-OCT, VG200S; SVision Imaging, Henan, China) examination, and dilated fundus examination. Corneal tomography, total corneal HOAs, and pupil diameters of the participants were analyzed through Pentacam (Pentacam HR type 70900). Cycloplegia was achieved with three drops of Mydrin-P (tropicamide 0.5%, phenylephrine HCl 0.5%; Santen Pharmaceutical, Shiga, Japan) at 5 min intervals [26], and performed before autorefractometry and fundus examination.

The study population consisted of 321 individuals aged 18–45 years (mean age: 28.4±6.25 years), of which 109 were male (33.9%) and 212 were female (66.1%). The participants were predominantly of Han Chinese ethnicity, and all had at least a secondary education level. The axial length thresholds were selected based on previous studies [24, 27, 28], which categorize mild (AL≤25 mm), moderate (AL>25 mm and <26 mm), and high myopia (AL≥26 mm) to investigate the effect of axial elongation on ocular structures, such as the choroid and HOAs. The right eye of each participant was selected for analysis.

Measurement of corneal higher-order aberrations

Corneal HOAs for a 6-mm pupil were measured using a high-resolution rotating Scheimpflug camera (Pentacam HR type 70900) in a scotopic environment (0.1 cd/m^2) through a natural pupil without dilation. The acquired data sets were expanded using a normalized sixth-order Zernike polynomial. The magnitudes of the coefficients of these Zernike polynomials are represented as the RMS and used to indicate wavefront aberrations. The HOAs included the following components: total HOA: Comprising third-to sixth-order terms; Spherical HOA: Represented by Z_4^0, Comatic HOA RMS: Comprising Z_3^{-1} and Z_3^1 combined; and Trefoil HOA RMS: Comprising Z_3^{-3} and Z_3^3 combined (Fig. 1). The measurements were repeated at least five times for each eye, and the three best-focused images were selected and averaged.

Measurement of choroidal parameters based on SS-OCT

To ensure consistency, SS-OCT (VG200S; SVision Imaging, Henan, China) measurements were taken between 13:30 to 17:00 to minimize the effects of diurnal variation on the measurements [29]. Eighteen radial scan lines, each measuring 12 mm in length, were employed for structural OCT scans centered on the fovea. A cutoff signal-strength index value≥6 was used as the inclusion criterion. The product was equipped with an eye-tracking system based on an integrated confocal scanning superluminescent ophthalmoscope (cSSO) to eliminate eye-motion artifacts. In addition, the current study corrected for AL before data analysis to minimize the effect of ocular magnification on measurements.

To compare the macular choroidal structure, we calculated the choroidal vascularity index (CVI) and choroidal thickness (CT) using both the horizontal and vertical lines from the 18 radial B-scans. The region between the choroid-sclera interface and retinal pigment epithelium–Bruch's membrane complex was defined as the choroid. Choroidal segmentation was performed semi-automatically using an algorithm implemented in MATLAB R2017 (MathWorks, Natick, MA, USA) and further refined manually by two trained examiners (KR and XZ). Any discrepancies between observers were resolved by a third adjudicator (DC). Following segmentation,

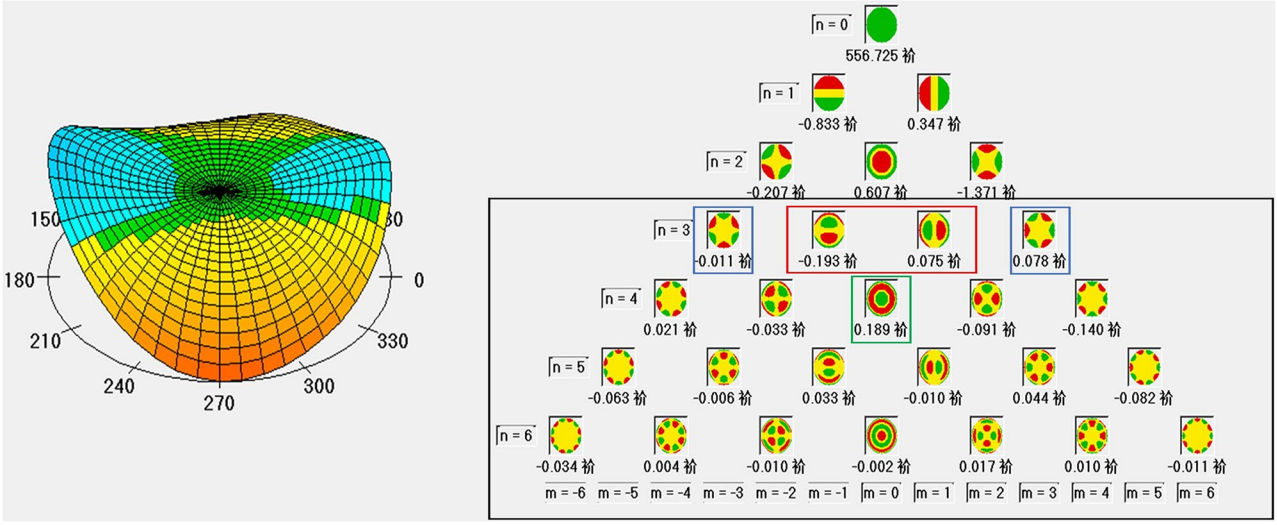

Fig. 1 Normalized sixth-order Zernike polynomials of aberrations based on corneal tomography examination (Pentacam HR type 70900). Black rectangle, higher-order aberrations; red rectangle, coma aberrations; blue rectangle, trefoil aberrations; green rectangle, spherical aberrations

each image was binarized to distinguish the luminal area (LA) and stromal region using Niblack's autolocal threshold [30]. After image processing, the total choroidal area (TCA), LA, and stromal area were determined. CVI was calculated using the LA/TCA ratio. To evaluate the reproducibility of choroidal segmentation between two trained examiners, we calculated the intraclass correlation coefficient (ICC) for both CT and CVI. The ICC values were 0.962 for mean CT and 0.973 for mean CVI, indicating excellent agreement between the examiners, thus supporting the reliability of the SS-OCT imaging data. The macular zone was further divided into regions consisting of three concentric rings with diameters of 1, 3, and 6 mm according to the ETDRS grid. The CVI and CT were assessed within each grid of the choroidal region (Fig. 2).

Statistical analysis

SPSS statistics (IBM, Armonk, NY, USA) was used for statistical analysis. To compare differences among the three groups, we used the $\chi 2$ test and analysis of variance test, as appropriate. Linear regression analysis was used to identify the associations between choroidal parameters and HOA variables, as well as the relationship between spherical equivalent (SE), AL, and choroidal parameters. Multivariate linear regression models were used to explore the relationships among corneal HOAs, CVI, CT, SE, and AL. We ensured that the assumptions of linearity, normality, and homoscedasticity were met. Normality was assessed using the Shapiro-Wilk test, and homoscedasticity was checked with the Breusch-Pagan test. Parameters with P values <0.05 in the univariate analysis were included in the multivariate models. The significance level was set to $\alpha=0.05$.

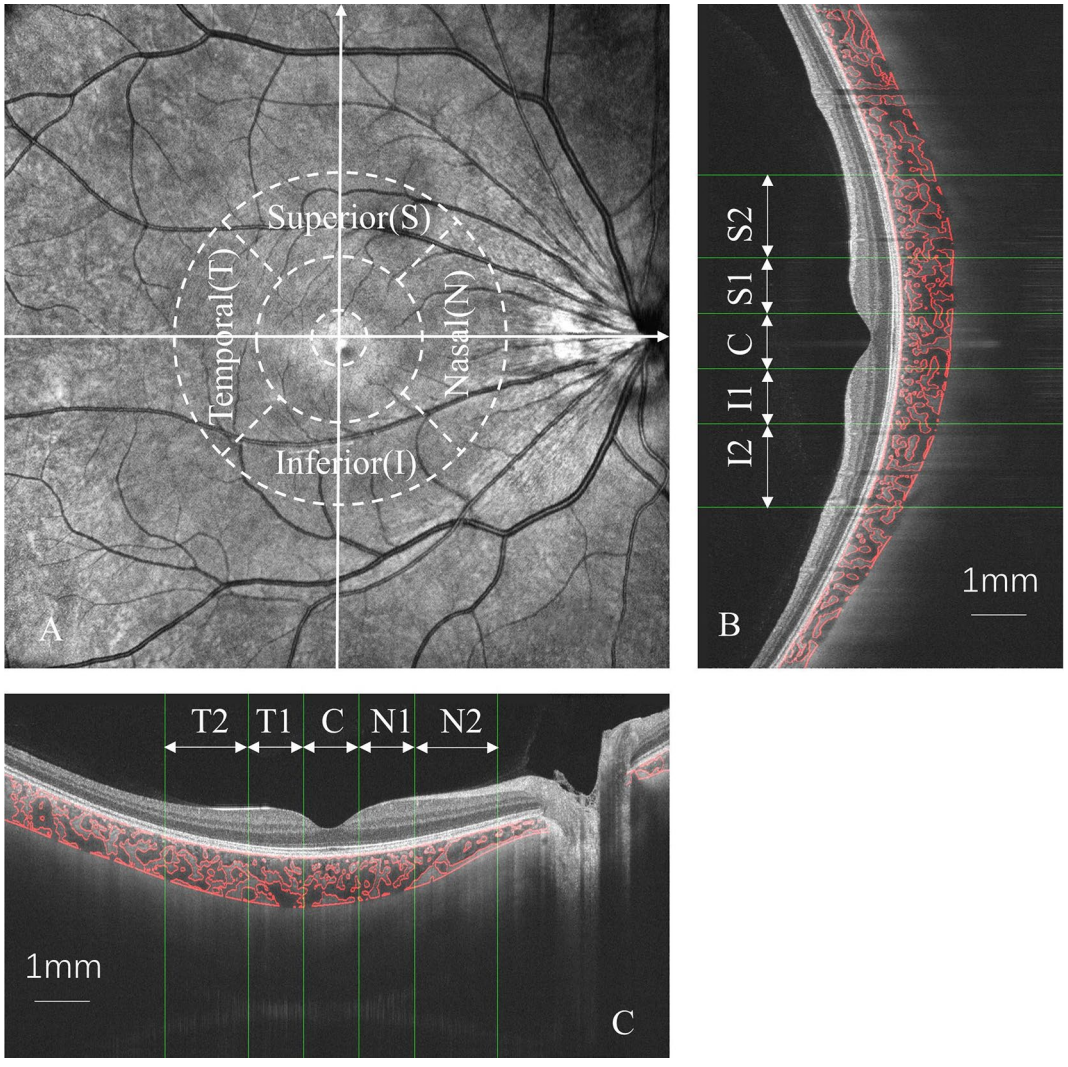

Fig. 2 Choroidal vascularity index (CVI) and choroidal thickness (CT) were measured in macular zone according to ETDRS grid (**A**). Both vertical (**B**) and horizontal (**C**) scans were measured using semi-automatic algorithms in MATLAB R2017a. T1, temporal parafovea; T2, temporal perifovea; N1, nasal parafovea; N2, nasal perifovea; I1, inferior parafovea; I2, inferior perifovea; S1, superior parafovea; S2, superior perifovea; C, center

Table 1 Baseline data in myopic eyes with different degrees of axial length

	Group 1	Group 2	Group3	*P* Value
Number	105	98	118	
Age, years	28.73 ± 5.87	28.92 ± 6.77	27.64 ± 6.08	0.274
Sex, male/female	25/80	36/62	48/70	< 0.05
SE, D	3.19 ± 1.94	4.54 ± 1.64	7.30 ± 2.25	< 0.001
Cylinder, D	0.59 ± 0.53	0.64 ± 0.52	0.92 ± 0.64	< 0.001
AL, mm	24.22 ± 0.57	25.51 ± 0.29	27.04 ± 0.91	< 0.001
IOP, mmHg	14.25 ± 2.52	13.93 ± 2.72	14.17 ± 2.79	0.684
CCT, um	526.79 ± 35.72	535.26 ± 26.66	534.53 ± 31.83	0.106
Pupil diameter, mm	3.22 ± 0.68	3.17 ± 0.55	3.35 ± 0.71	0.371

SE, spherical equivalent; AL, axial length; CCT, central corneal thickness

Table 2 Comparison of corneal wavefront aberrations in three groups

	Group1	Group2	Group3	*P* Value
Total RMS	1.50 ± 0.50	1.48 ± 0.59	1.52 ± 0.52	0.898
LOA RMS	1.44 ± 0.50	1.42 ± 0.59	1.45 ± 0.52	0.913
HOA RMS	0.42 ± 0.14	0.41 ± 0.13	0.39 ± 0.12	0.169
Spherical HOA RMS	0.21 ± 0.10	0.20 ± 0.08	0.18 ± 0.09†	< 0.05
Z_4^0	0.21 ± 0.11	0.20 ± 0.08	0.18 ± 0.10†	< 0.05
Comatic HOA RMS	0.23 ± 0.12	0.23 ± 0.14	0.21 ± 0.11	0.336
Z_3^{-1}	0.00 ± 0.19	-0.04 ± 0.23	-0.03 ± 0.20	0.44
Z_3^1	-0.16 ± 0.09‡	-0.10 ± 0.10	-0.08 ± 0.10†	< 0.001
Trefoil HOA RMS	0.15 ± 0.09	0.16 ± 0.11	0.15 ± 0.09	0.512
Z_3^{-3}	-0.07 ± 0.13	-0.08 ± 0.14	-0.06 ± 0.12	0.481
Z_3^3	0.03 ± 0.10	0.01 ± 0.11	0.01 ± 0.10	0.307

RMS, root mean square; LOA, lower-order aberrations; HOA, higher-order aberrations

† Significant differences between group 1 and group 3

‡ Significant differences between group 1 and group 2

Results

As indicated in Table 1, the study comprised 321 eyes from 321 individuals, with AL ranging from 22.55 mm to 31.28 mm (mean: 25.65 ± 1.35 mm) and SE spanning from +0.50 D to -15.63 D (mean: -5.11 ± 2.64 D). The mean age was 28.40 ± 6.25 years (range from 18 to 45 years). Of these, 109 were male and 212 were female. There were no significant differences in IOP or central corneal thickness among the three groups ($P > 0.05$). We found no significant differences in pupil diameters among groups ($p = 0.371$). This consistency in pupil size ensures that the corneal HOAs data presented are comparable across groups.

As there were significant differences in sex distribution between groups 1 and 3, we randomly selected 50 (25 men and 25 women) and 96 (48 men and 48 women) participants from groups 1 and 3, respectively. The results showed no differences in the corneal HOAs and choroid parameters between men and women.

Table 2 depicts the results of the comparison of corneal HOAs in the myopic groups, including Zernike coefficients and RMS values. There were significant differences in the spherical HOA RMS, Z_4^0, and Z_3^1 values among the three groups. Group 3 had lower spherical HOA RMS (0.18 ± 0.09 vs. 0.21 ± 0.10, $p = 0.046$) and Z_4^0 (0.18 ± 0.10 vs. 0.21 ± 0.11, $p = 0.035$) values than group 1. Group 1 showed lower Z_3^1 (-0.16 ± 0.09) value than groups 2 and 3 (-0.10 ± 0.10 and −0.08 ± 0.10, respectively, $p < 0.001$).

Table 3 shows a comparison of choroidal parameters, including CVI and CT, between the myopic groups. Mean, central, and I2 CVI values in the vertical scan were higher in groups 1 and 2 ($P < 0.01$) than those in group 3. Group 1 had a higher vertical CVI in the S1 region than group 3 ($P < 0.05$). Except for the N2 region, group 3 had a lower horizontal CVI than groups 1 and 2 ($P < 0.05$). The mean and all regions of CT decreased with an increase in AL, both vertically and horizontally ($P < 0.001$).

Table 4 displays the relationships between corneal HOAs and the mean CVI and CT. According to univariate and multivariate analysis, the comatic (Z_3^1) and trefoil (Z_3^3) components were strong predictors of the mean CVI of horizontal scan (β = -0.125, $P = 0.033$; β = 0.147, $P = 0.013$, respectively). Z_3^1 demonstrated a significant relationship with mean CT in both vertical (β = -0.178; $P = 0.002$) and horizontal lines (β = -0.166; $P = 0.007$).

Table 5 illustrates the correlations between SE, AL, and the choroidal parameters. According to the univariate linear regression analysis, except for the horizontal CVI in the N2 region, the mean values and all regions for both the CVI and CT were associated with SE and AL ($p < 0.01$). However, only the I2 and T2 regions of the CVI showed significant correlations with SE and AL in the multiple linear regression model ($p < 0.01$).

Discussion

In the current study, we characterized the differences in HOAs, CVI, and CT according to AL elongation. Our findings revealed that eyes with a longer AL had lower absolute values of SA and horizontal coma, as well as a decrease in choroidal vascularity and thickness. A correlation between choroidal perfusion and thickness with horizontal coma was demonstrated (Fig. 3, ACD). Additionally, the trefoil correlated with the mean CVI of the horizontal scan (Fig. 3, B). This finding implies a potential

Table 3 Comparison of CVIs and CTs in macular zone among three groups

Parameters		Group1	Group2	Group3	P Value
CVI (%)	Vertical Scan				
	Mean	61.04 ± 3.00	60.52 ± 3.69*	59.30 ± 4.56†	< 0.01
	I2	62.45 ± 4.69	61.62 ± 4.61*	59.91 ± 6.66†	< 0.01
	I1	60.94 ± 4.68	60.82 ± 5.95	59.56 ± 5.97	0.121
	C	60.44 ± 4.97	60.26 ± 6.41*	58.58 ± 6.73†	< 0.05
	S1	61.40 ± 4.34	59.99 ± 5.73	59.63 ± 5.65†	< 0.05
	S2	60.11 ± 3.70	60.05 ± 4.13	59.14 ± 5.29	0.193
	Horizontal Scan				
	Mean	59.94 ± 3.40	59.66 ± 3.67*	57.33 ± 4.20†	< 0.001
	N2	60.05 ± 4.20	60.87 ± 4.43	59.61 ± 5.28	0.145
	N1	60.40 ± 4.69	60.48 ± 5.15*	58.69 ± 5.02†	< 0.05
	C	60.40 ± 4.42	60.28 ± 5.35*	57.73 ± 6.52†	< 0.001
	T1	61.41 ± 6.37	60.56 ± 6.61*	57.05 ± 6.67†	< 0.001
	T2	57.78 ± 6.64	56.25 ± 6.75*	52.45 ± 6.65†	< 0.001
CT (um)	Vertical Scan				
	Mean	324.97 ± 83.54‡	276.33 ± 70.02*	228.34 ± 56.55†	< 0.001
	I2	315.07 ± 89.00‡	269.64 ± 79.12*	217.66 ± 63.47†	< 0.001
	I1	325.76 ± 88.19‡	274.53 ± 78.87*	217.86 ± 60.09†	< 0.001
	C	324.73 ± 90.69‡	271.00 ± 74.60*	218.16 ± 62.14†	< 0.001
	S1	327.84 ± 84.92‡	279.76 ± 73.27*	233.66 ± 60.62†	< 0.001
	S2	332.63 ± 90.31‡	285.51 ± 72.65*	249.27 ± 66.61†	< 0.001
	Horizontal Scan				
	Mean	301.14 ± 79.02‡	254.72 ± 63.50*	210.56 ± 50.68†	< 0.001
	N2	324.36 ± 81.66‡	285.11 ± 72.83*	236.28 ± 58.02†	< 0.001
	N1	341.13 ± 86.20‡	294.82 ± 74.10*	241.30 ± 58.57†	< 0.001
	C	327.42 ± 89.15‡	275.44 ± 75.47*	223.28 ± 62.88†	< 0.001
	T1	293.51 ± 86.55‡	241.65 ± 66.91*	200.80 ± 56.98†	< 0.001
	T2	238.88 ± 83.09‡	192.57 ± 60.59*	162.41 ± 57.71†	< 0.001

CVI, choroidal vascularity index; CT, choroidal thickness

*Significant differences between group 2 and group 3

† Significant differences between group 1 and group 3

‡ Significant differences between group 1 and group 2

link between optical quality and ocular perfusion in myopia. These findings hold significant potential for myopia management, especially in the development of personalized treatment approaches.

Knowledge of the specific HOAs in an individual's eyes allows for more personalized and precise eyeglasses and contact lenses. [12, 13] For example, a recently patented control lens was shown to retard AL elongation by solely inducing HOAs to generate blur signals on the retina [8]. Moreover, in refractive surgery procedures such as LASIK or PRK, understanding the specific HOAs in a patient's eyes allows surgeons to customize the procedure to address not only basic refractive errors but also these aberrations. Customization can improve postoperative outcomes and patient satisfaction. [26]

We found that the absolute values of SA and horizontal coma were lower in patients with a longer AL. This finding is consistent with those of other studies. Eyes with lower AL have larger angle kappas and show elevated levels of horizontal coma in the anterior cornea [31]. Oshika et al. observed an increase in coma-like aberrations following orthokeratology, suggesting a potential mechanism for controlling ocular axial growth [14]. Xu et al. demonstrated a negative association between comatic HOAs and axial elongation in myopic school children and adolescents [12]. These results prove the intervention of HOAs in myopia progression. However, some studies in adults have reported significantly higher levels of HOA RMS in myopic eyes than in emmetropic eyes [9, 32], while others have found no difference [10]. We speculated that the various measurement techniques and instruments utilized, as well as the patient characteristics, account for the broad inconsistencies between studies. The current study provides a reference for the distribution of corneal HOAs in young myopic patients. Further validation through longitudinal studies and establishing correlations between choroidal perfusion, thickness, and corneal coma is warranted.

Corneal HOAs may affect the choroid via the following mechanisms. First, because the human eye is an optical

Table 4 Linear regression analysis to determine the correlations between Mean CVI, CT and corneal HOAs

		Vertical Scan								Horizontal Scan							
		Univariate Analysis				Multivariate Analysis				Univariate Analysis				Multivariate Analysis			
	HOA Parameters	B	β	95%CI	P Value	B	β	95%CI	P Value	B	β	95%CI	P Value	B	β	95%CI	P Value
Mean CVI (%)	Total HOA RMS	0.064	0.002	-3.555 ~ 3.682	0.973					3.061	0.097	-0.565 ~ 6.686	0.099				
	Spherical HOA RMS	1.717	0.039	-3.353 ~ 6.787	0.507					6.234	0.141	1.175 ~ 11.294	< 0.05	4.862	0.11	-23.934 ~ 33.659	0.741
	Z_4^0	1.453	0.035	-3.412 ~ 6.318	0.559					5.983	0.141	1.129 ~ 10.837	< 0.05	1.786	0.042	-25.855 ~ 29.428	0.899
	Comatic HOA RMS	0.318	0.01	-3.387 ~ 4.022	0.867					2.609	0.081	-1.110 ~ 6.328	0.17				
	Z_3^{-1}	-0.097	-0.005	-2.319 ~ 2.125	0.932					-0.949	-0.049	-3.189 ~ 1.291	0.407				
	Z_3^1	-4.703	-0.122	-9.140 ~ -0.266	< 0.05	-4.018	-0.104	-8.502 ~ 0.467	0.08	-5.82	-0.15	-10.270 ~ -1.369	< 0.05	-4.868	-0.125	-9.326 ~ -0.410	< 0.05
	Trefoil HOA RMS	-1.365	-0.033	-6.195 ~ 3.464	0.58					2.915	0.069	-1.942 ~ 7.773	0.24				
	Z_3^{-3}	-2.686	-0.088	-6.198 ~ 0.827	0.135					-2.268	-0.074	-5.808 ~ 1.273	0.21				
	Z_3^3	4.74	0.123	0.308 ~ 9.173	< 0.05	4.064	0.105	-0.417 ~ 8.545	0.077	6.125	0.158	1.683 ~ 10.567	< 0.01	5.701	0.147	1.248 ~ 10.155	< 0.05
Mean CT (um)	Total HOA RMS	65.883	0.112	-2.124 ~ 133.891	0.059					77.419	0.14	13.935 ~ 140.903	< 0.05	25.605	0.046	-47.558 ~ 98.768	0.493
	Spherical HOA RMS	125.496	0.151	30.238 ~ 220.754	< 0.05	400.73	0.482	-141.245 ~ 942.705	0.148	123.578	0.16	34.898 ~ 212.259	< 0.01	315.101	0.407	-221.142 ~ 851.344	0.25
	Z_4^0	112.235	0.141	20.740 ~ 203.731	< 0.05	-268.688	-0.337	-788.540 ~ 251.164	0.312	111.024	0.15	25.812 ~ 196.237	< 0.05	-201.59	-0.272	-703.921 ~ 300.740	0.432
	Comatic HOA RMS	69.087	0.114	-0.579 ~ 138.753	0.053					64.955	0.115	-0.199 ~ 130.108	0.052				
	Z_3^{-1}	2.93	0.008	-39.090 ~ 44.951	0.891					4.43	0.013	-34.949 ~ 43.810	0.826				
	Z_3^1	-128.062	-0.174	-211.907 ~ -44.217	< 0.01	-130.748	-0.178	-213.983 ~ -47.513	< 0.01	-110.126	-0.162	-188.140 ~ -32.113	< 0.01	-108.896	-0.16	-187.509 ~ -30.283	< 0.01
	Trefoil HOA RMS	16.116	0.02	-75.317 ~ 107.549	0.73					41.808	0.057	-43.570 ~ 127.187	0.338				
	Z_3^{-3}	-11.607	-0.02	-78.279 ~ 55.066	0.733					-28.652	-0.053	-90.924 ~ 33.621	0.368				
	Z_3^3	70.13	0.096	-13.986 ~ 154.246	0.103					67.194	0.099	-11.448 ~ 145.835	0.095				

CVI, choroidal vascularity index; CT, choroidal thickness; RMS, root mean square; HOA, higher-order aberrations

Table 5 Linear regression between the Choroidal parameters and SE and AL in myopic patients

		Spherical Equivalent (D)								Axial Length (mm)							
		Univariate Analysis				Multivariate Analysis				Univariate Analysis				Multivariate Analysis			
Choroidal Parameters		B	β	95%CI	P Value	B	β	95%CI	P Value	B	β	95%CI	P Value	B	β	95%CI	P Value
CVI (%)	Vertical Scan																
	Mean	-0.172	-0.255	-0.244 ~ -0.101	< 0.001					-0.099	-0.285	-0.135 ~ -0.062	< 0.001				
	I2	-0.12	-0.254	-0.171 ~ -0.070	< 0.001	-0.1	-0.21	-0.159 ~ -0.041	< 0.01	-0.068	-0.282	-0.094 ~ -0.043	< 0.001	-0.056	-0.232	-0.086 ~ -0.027	< 0.001
	I1	-0.073	-0.155	-0.124 ~ -0.022	< 0.01	-0.008	-0.017	-0.074 ~ 0.058	0.81	-0.043	-0.176	-0.069 ~ -0.016	< 0.01	-0.004	-0.018	-0.038 ~ 0.029	0.794
	C	-0.066	-0.154	-0.113 ~ -0.020	< 0.01	-0.013	-0.03	-0.074 ~ 0.048	0.673	-0.039	-0.178	-0.063 ~ -0.015	< 0.01	-0.008	-0.038	-0.039 ~ 0.022	0.591
	S1	-0.082	-0.166	-0.136 ~ -0.029	< 0.01	-0.034	-0.069	-0.103 ~ 0.034	0.329	-0.049	-0.193	-0.076 ~ -0.022	< 0.001	-0.022	-0.086	-0.057 ~ 0.013	0.218
	S2	-0.086	-0.147	-0.150 ~ -0.022	< 0.01	-0.006	-0.01	-0.080 ~ 0.068	0.871	-0.048	-0.16	-0.081 ~ -0.016	< 0.01	-0.001	-0.004	-0.039 ~ 0.036	0.947
	Horizontal Scan																
	Mean	-0.211	-0.318	-0.281 ~ -0.142	< 0.001					-0.12	-0.352	-0.155 ~ -0.085	< 0.001				
	N2	-0.057	-0.101	-0.118 ~ 0.005	0.072					-0.041	-0.141	-0.072 ~ -0.009	< 0.05	-0.018	-0.063	-0.049 ~ 0.013	0.256
	N1	-0.084	-0.16	-0.141 ~ -0.027	< 0.01	-0.001	-0.001	-0.067 ~ 0.066	0.986	-0.046	-0.171	-0.075 ~ -0.017	< 0.01	0.007	0.028	-0.027 ~ 0.042	0.675
	C	-0.102	-0.218	-0.152 ~ -0.052	< 0.001	-0.032	-0.069	-0.097 ~ 0.033	0.331	-0.058	-0.243	-0.083 ~ -0.033	< 0.001	-0.02	-0.085	-0.053 ~ 0.013	0.228
	T1	-0.107	-0.277	-0.148 ~ -0.067	< 0.001	-0.037	-0.095	-0.090 ~ 0.017	0.18	-0.061	-0.308	-0.082 ~ -0.040	< 0.001	-0.022	-0.113	-0.050 ~ 0.005	0.107
	T2	-0.13	-0.346	-0.168 ~ -0.091	< 0.001	-0.102	-0.272	-0.147 ~ -0.057	< 0.001	-0.07	-0.367	-0.090 ~ -0.051	< 0.001	-0.053	-0.276	-0.076 ~ -0.030	< 0.001
CT (um)	Vertical Scan																
	Mean	-0.018	-0.564	-0.021 ~ -0.015	< 0.001					-0.009	-0.537	-0.011 ~ -0.007	< 0.001				
	I2	-0.015	-0.506	-0.018 ~ -0.012	< 0.001	-0.001	-0.044	-0.009 ~ 0.006	0.723	-0.068	-0.282	-0.094 ~ -0.043	< 0.001	-0.002	-0.098	-0.005 ~ 0.002	0.443
	I1	-0.016	-0.54	-0.019 ~ -0.013	< 0.001	-0.003	-0.11	-0.016 ~ 0.009	0.608	-0.043	-0.176	-0.069 ~ -0.016	< 0.01	-0.002	-0.126	-0.008 ~ 0.005	0.562
	C	-0.017	-0.552	-0.019 ~ -0.014	< 0.001	-0.003	-0.115	-0.017 ~ 0.010	0.615	-0.039	-0.178	-0.063 ~ -0.015	< 0.01	-0.004	-0.287	-0.011 ~ 0.003	0.217
	S1	-0.018	-0.559	-0.021 ~ -0.015	< 0.001	-0.007	-0.228	-0.019 ~ 0.005	0.238	-0.008	-0.52	-0.010 ~ -0.007	< 0.001	-0.001	-0.091	-0.008 ~ 0.005	0.644
	S2	-0.016	-0.518	-0.019 ~ -0.013	< 0.001	-0.003	-0.096	-0.010 ~ 0.004	0.395	-0.007	-0.454	-0.009 ~ -0.006	< 0.001	0.001	0.04	-0.003 ~ 0.004	0.728
	Horizontal Scan																
	Mean	-0.02	-0.559	-0.023 ~ -0.016	< 0.001					-0.01	-0.55	-0.012 ~ -0.008	< 0.001				
	N2	-0.017	-0.513	-0.020 ~ -0.014	< 0.001	-0.002	-0.054	-0.010 ~ 0.007	0.674	-0.009	-0.504	-0.010 ~ -0.007	< 0.001	-0.002	-0.137	-0.007 ~ 0.002	0.295
	N1	-0.018	-0.559	-0.020 ~ -0.015	< 0.001	-0.007	-0.21	-0.022 ~ 0.008	0.391	-0.009	-0.536	-0.010 ~ -0.007	< 0.001	-0.001	-0.05	-0.009 ~ 0.007	0.839
	C	-0.017	-0.562	-0.020 ~ -0.014	< 0.001	-0.005	-0.178	-0.020 ~ 0.009	0.459	-0.058	-0.243	-0.083 ~ -0.033	< 0.001	-0.004	-0.267	-0.012 ~ 0.003	0.273
	T1	-0.018	-0.538	-0.021 ~ -0.015	< 0.001	-0.006	-0.179	-0.017 ~ 0.005	0.311	-0.009	-0.522	-0.010 ~ -0.007	< 0.001	-0.001	-0.046	-0.007 ~ 0.005	0.797
	T2	-0.016	-0.452	-0.019 ~ -0.012	< 0.001	0.001	0.037	-0.006 ~ 0.008	0.713	-0.008	-0.466	-0.010 ~ -0.007	< 0.001	-0.002	-0.086	-0.005 ~ 0.002	0.405

CVI, choroidal vascularity index; CT, choroidal thickness

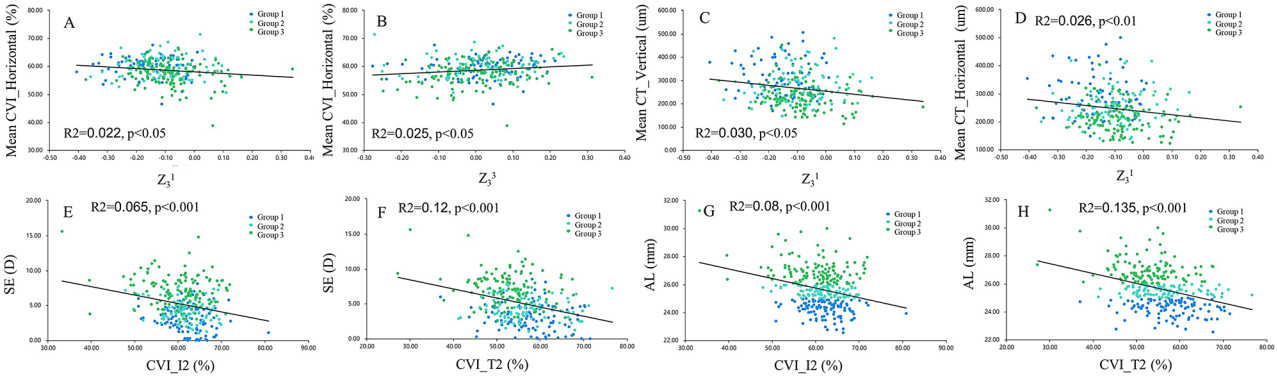

Fig. 3 Scatterplots showing the relationships between the choroidal parameters and corneal higher-order aberrations (HOAs) (**A-D**), as well as the correlation of spherical equivalent (SE), axial length (AL), and choroid (**E-H**)

component system, a balance of aberrations between the optical elements is required. A compensatory mechanism has been previously reported to balance corneal horizontal coma, perhaps in the lens [31]. Furthermore, research indicates that aberration variation and accommodation are highly correlated [33], and long-term abnormal accommodation may be responsible for changes in choroidal structure [34, 35]. We also speculated that choroidal vascularity and thickness are components of the compensatory mechanism of corneal coma. Second, it is crucial to note that spherical and coma aberrations reduce retinal image quality and produce variations in optical vergence across the entrance pupil of the eye [36]. Thus, corneal HOAs may serve as optical signals contributing to the regulation of eye growth and development of refractive errors. Disturbances in retinal dopamine homeostasis are associated with choroidal blood perfusion in myopias [20, 37, 38]. Therefore, some pharmacological interventions for myopia aim to influence ocular structures, including the choroid.

Furthermore, in the multiple linear regression, a clear linear relationship was found between the CVI in regions I2, T2, and AL and SE (Fig. 3, E-H). Research has consistently shown that choroidal thinning is most pronounced temporally during the progression of myopia, likely owing to temporal stretching of the choroid and sclera [39]. It has been proposed that non-vascular smooth muscle cells and intrinsic choroidal neurons play a role in regulating choroidal structure, as they predominantly reside in the central and temporal quadrants of the choroid [40, 41]. Therefore, the temporal choroidal structure is more sensitive in myopic eyes. However, most choroidal studies have focused solely on horizontal scans and have provided limited information on vertical scans. Our results suggest that temporal and inferior CVI measured by SS-OCT with an algorithm can be an objective indicator for monitoring myopic development.

In this study, the CVI in the high myopia group was significantly lower than those in the low and moderate myopia groups. However, there was no significant difference in the CVI between groups 1 and 2. Notably, choroidal perfusion was positively correlated with AL, indicating that as the eye's AL increased, choroidal blood flow also increased. The changes observed in the high myopic eyes were more significant than those in the low myopic eyes. This suggests that CVI remains relatively stable in the early stages of myopia but experiences a significant decline in the intermediate and advanced stages. In contrast to the nearly linear relationship between CT and AL, the relationship between the choroidal vasculature and AL is complex.

This study had certain limitations. First, it was a cross-sectional study; therefore, changes in the HOAs and choroid during the progression of myopia could not be documented. Future longitudinal studies may be useful for overcoming this shortcoming. Second, although SA may change owing to age-related lens modifications [42], it is worth noting that all participants in this study were young myopia patients, and cataract patients were excluded. Third, while our findings suggest compensatory mechanisms involving the choroid and corneal HOAs, individual variability in these responses may be significant, and external factors such as environmental lighting, visual habits, and accommodation demands could influence outcomes. These factors should be considered in future studies to better understand the scope of these compensatory mechanisms.

Conclusions

In conclusion, lower absolute values of SA and horizontal coma were observed in longer AL myopic patients. Choroid alterations in myopic patients are correlated with corneal HOAs. Horizontal coma aberration was the most significant correlation factor. This study provides a reference for the characteristics of corneal HOAs and choroid in young myopic patients, and may help prevent and manage myopia. Future research should investigate the longitudinal effects of HOA modulation on choroidal

structure to better understand its potential role in personalized treatment plans for myopia management.

Acknowledgements
Not applicable.

Author contributions
Kaiming Ruan, Dan Cheng contributed to the conception of the study; Xueying Zhu, Fangjun Bao, Jun Zhu, and Fenfen Li performed the experiment; Kaiming Ruan, Xueying Zhu, Shiqi Sun, Fangjun Bao, Jun Zhu, Fenfen Li Meixiao Shen and Yufeng Ye performed the data analyses; Kaiming Ruan and Dan Cheng wrote the manuscript; Meixiao Shen and Yufeng Ye revised the manuscript.

Funding
This study was supported by research grants from the National Natural Science Foundation of China (No. 81900910), Natural Science Foundation of Zhejiang Province (No.LQ19H120003), Basic Scientific Research Project of Wenzhou (Y2023809, Y20190638).

Data availability
No datasets were generated or analysed during the current study.

Declarations

Ethics approval and consent to participate
The study protocol adhered to the tenets of the Declaration of Helsinki and was approved by the Ethics Committee of Wenzhou Medical University. All patients have been informed of the purpose of the experiment and signed informed consent.

Consent for publication
Not applicable.

Competing interests
The authors declare no competing interests.

Received: 28 August 2024 / Accepted: 7 November 2024
Published online: 15 November 2024

References

1. Morgan IG, Ohno-Matsui K, Saw S-M. Myopia Lancet (London England). 2012;379(9827):1739–48.
2. Holden BA, et al. Global prevalence of myopia and high myopia and temporal trends from 2000 through 2050. Ophthalmology. 2016;123(5):1036–42.
3. Bullimore MA, et al. The risks and benefits of Myopia Control. Ophthalmology. 2021;128(11):1561–79.
4. Wu P-C, et al. Myopia Prevention and Outdoor Light Intensity in a School-based Cluster Randomized Trial. Ophthalmology. 2018;125(8):1239–50.
5. Yam JC, et al. Three-year clinical trial of low-concentration atropine for myopia progression (LAMP) study: continued Versus Washout: phase 3 report. Ophthalmology. 2022;129(3):308–21.
6. Morgan IG, et al. The epidemics of myopia: Aetiology and prevention. Prog Retin Eye Res. 2018;62:134–49.
7. Howlett MHC, McFadden SA. Spectacle lens compensation in the pigmented guinea pig. Vision Res. 2009;49(2):219–27.
8. Liu X, et al. One-year myopia control efficacy of cylindrical annular refractive element spectacle lenses. Acta Ophthalmol. 2023;101(6):651–7.
9. Yazar S, et al. Comparison of monochromatic aberrations in young adults with different visual acuity and refractive errors. J Cataract Refract Surg. 2014;40(3):441–9.
10. Kwan WCK, Yip SP, Yap MKH. Monochromatic aberrations of the human eye and myopia. Clin Experimental Optometry. 2009;92(3):304–12.
11. Llorente L, et al. Myopic versus hyperopic eyes: axial length, corneal shape and optical aberrations. J Vis. 2004;4(4):288–98.
12. Xu Y, et al. Higher-order aberrations and their association with axial elongation in highly myopic children and adolescents. Br J Ophthalmol. 2023;107(6):862–8.
13. Chen C, et al. Higher-order aberrations and visual performance in myopic children treated with Aspheric Base curve-designed Orthokeratology. Volume 49. Eye & Contact Lens; 2023. pp. 71–6. 2.
14. Hiraoka T et al. Influence of ocular wavefront aberrations on axial length elongation in myopic children treated with overnight orthokeratology. Ophthalmology, 2015. 122(1).
15. Lau JK, et al. Higher-order aberrations and axial elongation in myopic children treated with Orthokeratology. Volume 61. Investigative Ophthalmology & Visual Science; 2020. p. 22. 2.
16. Hiraoka T, et al. Relationship between higher-order wavefront aberrations and natural progression of myopia in schoolchildren. Sci Rep. 2017;7(1):7876.
17. Wang D, et al. Optical Defocus rapidly changes Choroidal Thickness in Schoolchildren. PLoS ONE. 2016;11(8):e0161535.
18. Wu H, et al. Scleral hypoxia is a target for myopia control. Proc Natl Acad Sci USA. 2018;115(30):E7091–100.
19. Zhou X, et al. Increased choroidal blood perfusion can inhibit form deprivation myopia in Guinea Pigs. Investig Ophthalmol Vis Sci. 2020;61(13):25.
20. Zhou X, et al. Decreased Choroidal Blood Perfusion induces myopia in Guinea Pigs. Investig Ophthalmol Vis Sci. 2021;62(15):30.
21. Summers JA. The choroid as a sclera growth regulator. Exp Eye Res. 2013;114:120–7.
22. Hiraoka T et al. Influences of cycloplegia with topical atropine on ocular higher-order aberrations. Ophthalmology, 2013. 120(1).
23. Wu H, et al. Assessment of Choroidal Vascularity and Choriocapillaris Blood Perfusion in Anisomyopic adults by SS-OCT/OCTA. Investig Ophthalmol Vis Sci. 2021;62(1):8.
24. Cheng D, et al. Characteristics of the Optic nerve head in myopic eyes using swept-source Optical Coherence Tomography. Volume 63. Investigative Ophthalmology & Visual Science; 2022. p. 20. 6.
25. Wang Y, et al. Vascular changes of the Choroid and their correlations with visual acuity in pathological myopia. Investig Ophthalmol Vis Sci. 2022;63(12):20.
26. Sun YY et al. Cycloplegic refraction by 1% cyclopentolate in young adults: is it the gold standard? The Anyang University Students Eye Study (AUSES). Br J Ophthalmol, 2018.
27. Park KS, et al. Effect of axial length on peripapillary microvasculature: an optical coherence tomography angiography study. PLoS ONE. 2021;16(10):e0258479.
28. Wei L, et al. Contrast sensitivity function: a more sensitive index for assessing Protective effects of the Cilioretinal artery on Macular Function in high myopia. Volume 63. Investigative Ophthalmology & Visual Science; 2022. p. 25. 13.
29. Tan CS, et al. Diurnal variation of choroidal thickness in normal, healthy subjects measured by spectral domain optical coherence tomography. Investig Ophthalmol Vis Sci. 2012;53(1):261–6.
30. Sonoda S et al. Luminal and stromal areas of choroid determined by binarization method of optical coherence tomographic images. Am J Ophthalmol, 2015. 159(6).
31. Lu F, et al. On the compensation of horizontal coma aberrations in young human eyes. Ophthalmic Physiological Optics: J Br Coll Ophthalmic Opticians (Optometrists). 2008;28(3):277–82.
32. Paquin M-P, Hamam H, Simonet P. Objective measurement of optical aberrations in myopic eyes. Volume 79. Optometry and Vision Science: Official Publication of the American Academy of Optometry; 2002. pp. 285–91. 5.
33. Ke B, et al. The relationship between high-order aberration and anterior ocular Biometry during accommodation in young healthy adults. Investig Ophthalmol Vis Sci. 2017;58(13):5628–35.
34. Chang X, et al. Assessment of Choroidal Vascularity and Choriocapillaris Blood Perfusion after Accommodation in Myopia, Emmetropia, and Hyperopia groups among children. Front Physiol. 2022;13:854240.
35. Kaphle D, et al. Central and peripheral choroidal thickness and eye length changes during accommodation. Ophthalmic Physiological Optics: J Br Coll Ophthalmic Opticians (Optometrists). 2023;43(3):311–8.
36. Hughes RP, et al. Higher order aberrations, refractive error development and myopia control: a review. Clin Experimental Optometry. 2020;103(1):68–85.
37. Huemer K-H, et al. Effects of dopamine on retinal and choroidal blood flow parameters in humans. Br J Ophthalmol. 2007;91(9):1194–8.
38. Wei P, Han G, Wang Y. *Effects of dopamine D2 receptor antagonists on retinal pigment epithelial/choroid complex metabolism in form-deprived myopic guinea pigs.* Proteomics, 2023: p. e2200325.
39. Lee K, et al. Topographical variation of macular choroidal thickness with myopia. Acta Ophthalmol. 2015;93(6):e469–74.

40. May CA. Non-vascular smooth muscle cells in the human choroid: distribution, development and further characterization. J Anat. 2005;207(4):381–90.
41. Flügel C, et al. Species differences in choroidal vasodilative innervation: evidence for specific intrinsic nitrergic and VIP-positive neurons in the human eye. Investig Ophthalmol Vis Sci. 1994;35(2):592–9.
42. Amano S, et al. Age-related changes in corneal and ocular higher-order wavefront aberrations. Am J Ophthalmol. 2004;137(6):988–92.

Publisher's note